Light Curves of Supernova AT2023hpb

Department of Physics, University of California, Santa Barbara, CA

June 13th, 2023

Abstract

In our project, we focused on analyzing the light curves of a recently discovered supernova, AT2023hpb. Images of AT2023hpb were collected across i, g, and r filters during a 10-day interval by the Las Cumbres Observatory (LCO) upon requested. After aquiring the data, Astroart 8 software was used to analyze the magnitude (brightness) change throughout the period. We then employed Castro's equation to compute the uncertainty in our photometric measurements. The light curves, thus modeled, were then compared with theoretical projections corresponding to different types of supernova. We found an unexpected peak in the star's brightness towards the end of the observation period, leading us to categorize AT2023hpb as a Type II supernova. Nevertheless, the limited observation window presents a constraint, hindering the identification of a definitive pattern in the observed variability.

1 Introduction

A supernova is an astronomical event that occurs when a star explodes, which is considered the most substantial type of explosion in the cosmos. The onset of a supernova can be triggered by one of two different scenarios, both involving changes in the star's core. In a binary star system, one star (a carbon-oxygen white dwarf) pulls matter from its twin until it cannot handle the excess matter, leading to an explosion. Alternatively, a single star nearing the end of its life may transfer some of its mass to its core until the core's weight is too much for it to sustain, resulting in a supernova. However, stars like our sun do not have sufficient mass to undergo this process. [1]

Supernova are categorized by astronomers based on their light patterns and the specific absorption lines of various chemical elements observed in their spectra. When examining the spectrum of a supernova, the presence of hydrogen lines (referred to as the Balmer series in the visible part of the spectrum) determines its classification as Type II, while the absence of these lines leads to its classification as Type I. Within each of these two types, further subdivisions exist based on the presence of lines from other elements or the shape of the supernova's light curve, which plots its apparent brightness over time. [2]

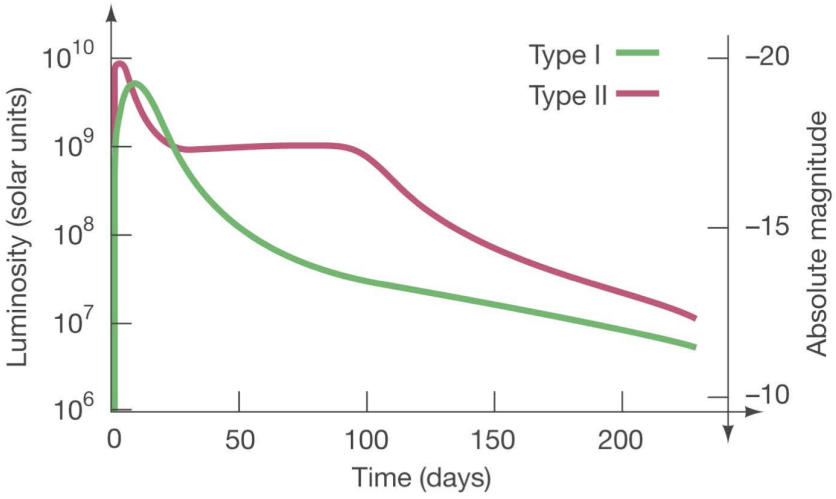

Figure 1: Comparison of the light curves of Type I and Type II supernovae. [3]

Type I supernovae are further categorized based on their spectra. Type Ia supernovae

show a distinct absorption line caused by ionized silicon. On the other hand, Type Ib and Type Ic supernovae lack this specific strong line. Instead, Type Ib supernovae display prominent neutral helium lines, while Type Ic supernovae do not. In the past, the light curves of Type I supernovae were generally considered quite similar, making it challenging to make meaningful distinctions between them. [4]

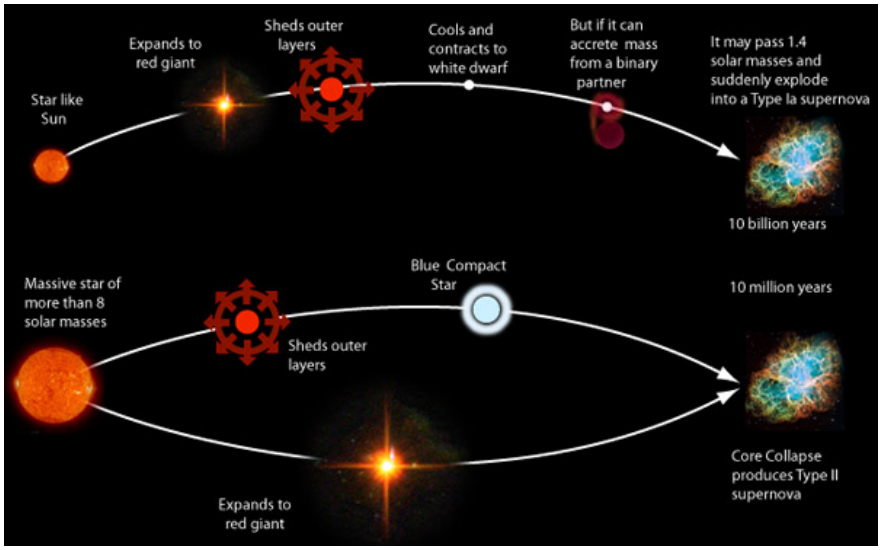

Figure 2: The formation of Type Ia and Type II supernova. [5]

Similarly, Type II Supernovae can also be further categorized based on their spectra. While the majority of Type II supernovae exhibit broad emission lines, indicating high expansion velocities of several thousand kilometers per second, there are exceptions like SN 2005gl that display narrower features in their spectra. These particular cases are known as Type IIn supernovae, with the "n" representing "narrow." Type II supernovae with normal spectra characterized by broad hydrogen lines that persist throughout the decline phase are classified based on their light curves. The most common type exhibits a distinctive "plateau" in the light curve, where the visual brightness remains relatively constant for several months before the decline resumes. These are referred to as Type II-P supernovae, indicating the presence of a plateau. Type II-L supernovae, which are less common, lack a distinct plateau. The "L" designation signifies "linear," although the light curve does not follow a perfectly straight line. [2]

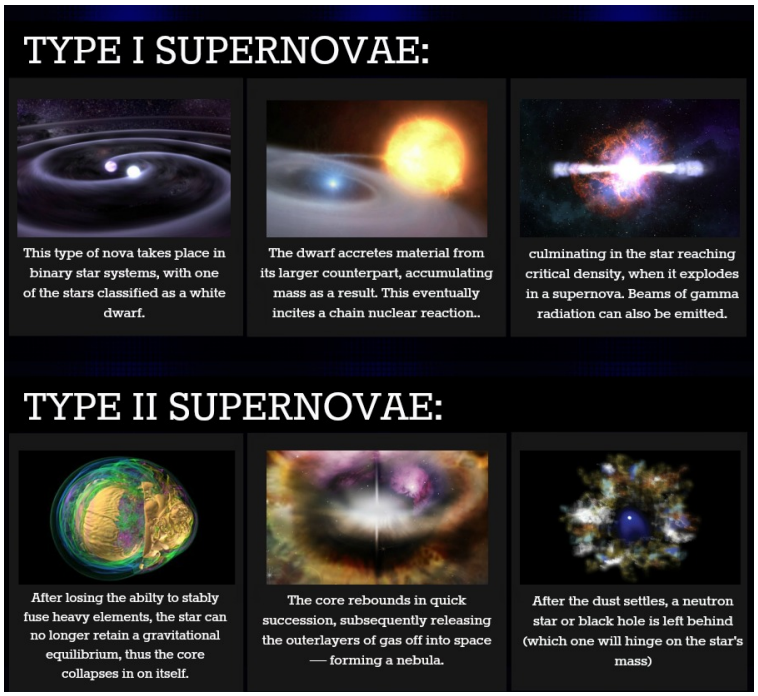

Figure 3: The classification of supernovae. Image Credits (Clockwise, from top to bottom): Tod Strohmayer and Dana Berry, Celojums Kosmosa (Vimeo), NASA/Dana Berry/Skyworks Digital, NASA (taken by Chandra).'Daftopia' (Deviant Art), Argonne National Laboratory/Hongfeng Yu. (nfographic by' Prom Quarks to Quasars)

The distinctive characteristics of Type II supernovae, whether they exhibit narrow features, a distinctive "plateau," or a linear decline in brightness, are all related to the complex interplay of the initial explosion, the materials ejected, and the underlying energy sources. In particular, the persistence of the supernova's visible glow over several months is a key factor that astronomers have extensively studied to better understand these celestial events. The gases ejected from the supernova would lose brightness rapidly if there wasn't an external energy source to keep them hot. Initially, the origin of this energy, which sustains the visible glow of the supernova for several months, posed a perplexing question. Some scientists speculated that the rotational energy from the pulsar at the center could serve as this energy source. [6] Even though the energy responsible for the creation of each type of supernova is delivered promptly, the subsequent light curves are primarily influenced by the ongoing radioactive heating of the rapidly expanding ejected materials. The highly radioactive nature of the expelled gases was initially determined through meticulous nucleosynthesis

calculations in the late 1960s. Subsequently, this prediction has been confirmed as accurate for the majority of supernovae. [7] The definitive identification of the primary radioactive nuclei was made possible only with the direct observation of gamma-ray lines in the case of SN 1987A. [8]

Scientists study supernovas for their invaluable insights into the universe. For instance, one type of supernova has revealed that our universe is not only expanding but also at an accelerating rate. Additionally, supernovas are vital for spreading elements across the universe, as the explosion propels elements and debris into space. Many elements found on Earth originate from the cores of stars and continue to contribute to the formation of new celestial bodies. [1]

Target Name	RA (J2000)	Dec (J2000)	Filter	# Exposures	Integration Time (s)	Observational Windows
AT 2023hpb	00:51:11.790	-73:11:30.30	SDSS g'	2	100	ASAP Every two days (repeat observation for two weeks)
AT 2023hpb	00:51:11.790	-73:11:30.30	SDSS i'	2	100	ASAP Every two days (repeat observation for two weeks)
AT 2023hpb	00:51:11.790	-73:11:30.30	SDSS r'	2	100	ASAP Every two days (repeat observation for two weeks)

Figure 4: Our initial observation request to LCO

2 Methods

Our project focuses on the cataclysmic variable star AT2023hpb, a part of a binary star system where a white dwarf accumulates matter from an accompanying star. We used the photometric analysis of AT2023hpb through a Global Telescope Network at LCO. Images were captured using the SBIG STL-6303 instrument with a 0.4-meter telescope, equipped

with a Charge-coupled Device (CCD), translates visual data into digital images. It exhibits a readout noise level of 14.5 electrons, a gain of 1.6 electrons per ADU, and a dark current of 0.03 electrons per pixel per second. The photometric analysis employed Astroart 8 software, specifically its Star Atlas feature, which displays star positions and carries out astrometric or photometric calibration of a single image. Reference stars were identified using the GAIA DR3 star catalog, which is based on data collected by the Gaia space telescope.

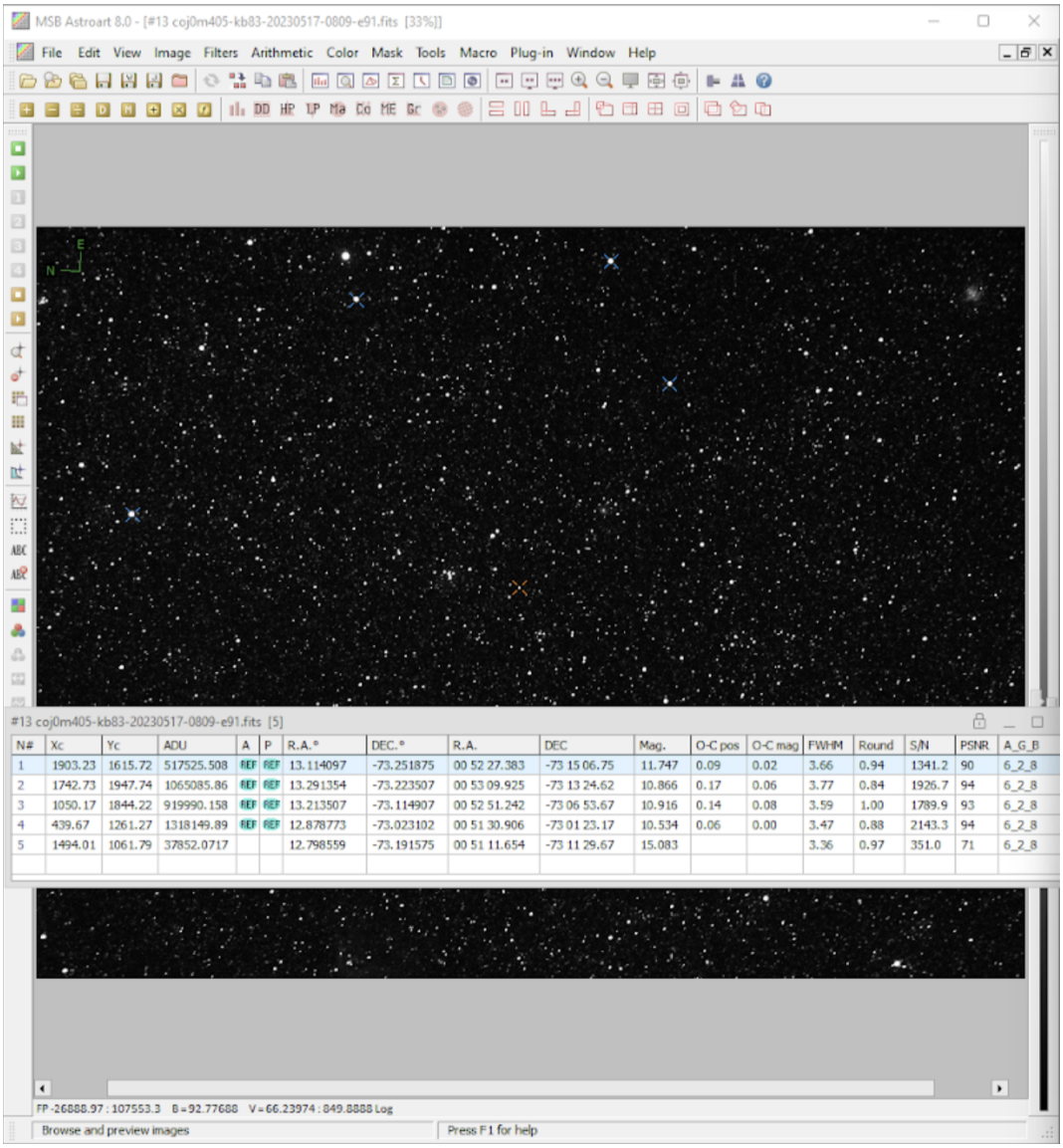

N#	Xc	Yc	ADU	A	P	R.A.°	DEC.°	R.A.	DEC	Mag.	O-C pos	O-C mag	FWHM	Round	S/N	PSNR	A_G_B
1	1903.23	1615.72	517525.508	REF	REF	13.114097	-73.251875	00 52 27.383	-73 15 06.75	11.747	0.09	0.02	3.66	0.94	1341.2	90	6_2_8
2	1742.73	1947.74	1065085.86	REF	REF	13.291354	-73.223507	00 53 09.925	-73 13 24.62	10.866	0.17	0.06	3.77	0.84	1926.7	94	6_2_8
3	1050.17	1844.22	919990.158	REF	REF	13.213507	-73.114907	00 52 51.242	-73 06 53.67	10.916	0.14	0.08	3.59	1.00	1789.9	93	6_2_8
4	439.67	1261.27	1318149.89	REF	REF	12.878773	-73.023102	00 51 30.906	-73 01 23.17	10.534	0.06	0.00	3.47	0.88	2143.3	94	6_2_8
5	1494.01	1061.79	37852.0717			12.798559	-73.191575	00 51 11.654	-73 11 29.67	15.083			3.36	0.97	351.0	71	6_2_8

Figure 5: The 4 reference stars we picked

AT2023hpb was initially discovered on May 1, 2023, at the coordinates R.A. = 00h51m11s.790,

Decl. = -73°11'30".30, with a 14.2 magnitude. This supernova was chosen for observation due to its suitable magnitude for detailed study and analysis. We scheduled two 100-second exposures for each of the SDSS i', SDSS r', and SDSS g' filters. We planned our observational period to span every two days, repeating this process over two weeks. We received observational data between May 10th and 20th, except the 12th, with 4 images for every filter each day, 120 images in total. The images from May 20 proved to be unusable, leaving us with useful data from the preceding nine days. It should be noted that the images were not all captured from the same observational locations.

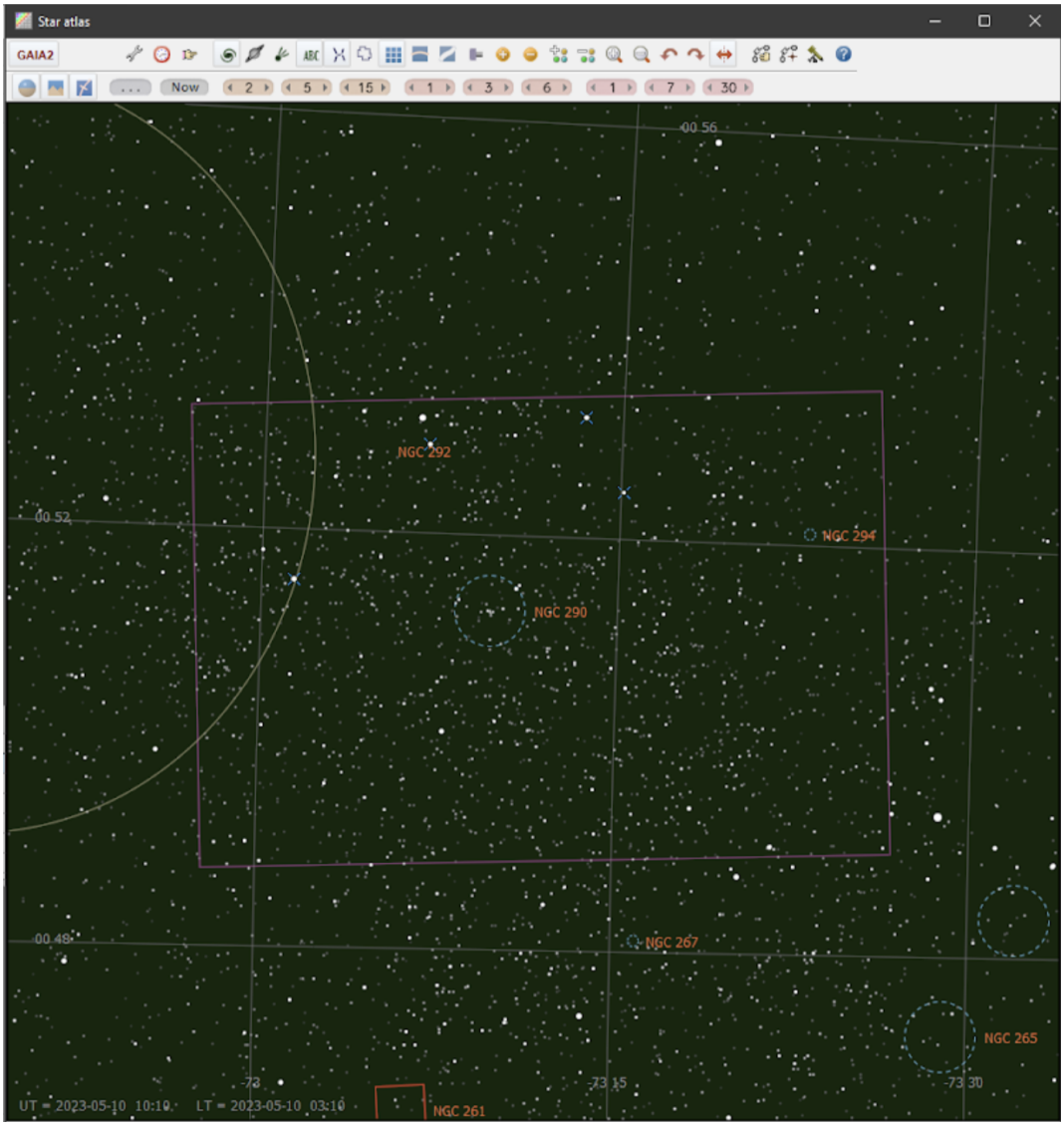

Figure 6: Astrometry using Star Atlas with GAIA DR2 catalog

We used Astroart 8 for our photometric analysis, aiming to chart the apparent magnitude of the supernova AT2023hpb through various filters on a daily basis. Given that we had two exposures for each filter every day, we choose the one with better signal-to-noise ratio (SNR). For photometry, we selected 4 bright, easy-to-find stars from the image as our reference points, as shown in Figure 5.

The same 4 stars were used across all images. The GAIA DR2 catalog was used for Star Atlas as our reference. After executing the astrometry, Star Atlas pinpointed the locations of the reference stars near NGC 290, depicted in Figure 6. The photometry process then derived AT2023hpb's magnitude, using the reference stars. Using the same process, we obtained the magnitude of AT2023hpb in each image.

3 Results

3.1 Raw Data

The raw data and the derived magnitude of AT2023hpb is shown in Figure 7.

For the abbreviations in Figure 7, FWHM is Full Width at Half Maximum; Round is the ratio of Minor axis and Major axis of the FWHM; S/N is the SNR; PNSR is a metric that measure the noise on the image.

Filter	Date	Magnitude	O-C pos	O-C mag	FWHM	Round	S/N	PNSR	A_G_B	Magnitude
i blue	May 10 (LSC)	14.257			3.81	0.89	200.4	67	6_2_8	-14.257
	May 11 (LSC)	14.377			3.66	0.91	188.5	65	6_2_8	-14.377
	May 13 (LSC)	14.389			4.06	0.99	206.3	67	6_2_8	-14.389
	May 14 (LSC)	14.38			4.30	0.81	193.3	64	6_2_8	-14.38
	May 15 (LSC)	14.493			4.94	0.9	185.1	65	6_2_8	-14.493
	May 16 (LSC)	14.584			4.39	0.93	192.8	66	6_2_8	-14.584
	May 17 (COJ)	14.901			3.40	0.94	270.1	71	6_2_8	-14.901
	May 18 (LSC)	14.585			4.25	0.91	197	66	6_2_8	-14.585
	May 19 (COJ)	14.395			6.12	0.86	170.8	65	6_2_8	-14.395
	May 20 (LSC)	N/A							6_2_8	
g red	May 10 (LSC)	14.026			4.77	0.52	99.1	53	6_2_8	-14.026
	May 11 (LSC)	14.190			5.85	0.52	86.9	51	6_2_8	-14.190
	May 13 (LSC)	14.284			4.90	0.82	113.8	53	6_2_8	-14.284
	May 14 (LSC)	14.151			4.23	0.83	134.1	57	6_2_8	-14.151
	May 15 (LSC)	14.238			4.62	0.81	113.5	54	6_2_8	-14.238
	May 16 (LSC)	14.214			4.31	0.85	141.4	57	6_2_8	-14.214
	May 17 (COJ)	14.229			3.55	0.82	201.5	62	6_2_8	-14.229
	May 18 (LSC)	14.238			3.90	0.81	146.9	57	6_2_8	-14.238
	May 19 (COJ)	13.609			6.79	0.92	139.1	57	6_2_8	-13.609
	May 20 (LSC)	N/A								
r yellow	May 10 (LSC)	14.430			4.07	0.95	242.6	64	6_2_8	-14.430
	May 11 (LSC)	14.507			3.61	0.88	223.5	63	6_2_8	-14.507
	May 13 (LSC)	14.549			4.26	0.91	246.5	65	6_2_8	-14.549
	May 14 (LSC)	14.449			4.38	0.9	249	65	6_2_8	-14.449
	May 15 (LSC)	14.547			5.10	0.88	223.2	64	6_2_8	-14.547
	May 16 (LSC)	14.666			4.55	0.87	243.7	65	6_2_8	-14.666
	May 17 (LSC)	15.083			3.36	0.97	351	71	6_2_8	-15.083
	May 18 (COJ)	14.735			4.13	0.84	244.9	65	6_2_8	-14.735
	May 19 (COJ)	14.267			5.94	0.71	218.8	63	6_2_8	-14.267
	May 20 (LSC)	N/A							6_2_8	

Figure 7: The 4 reference stars we picked

3.2 Error Analysis

Given SNR equation below:

$$\frac{S}{N} = \frac{FA_\varepsilon\sqrt{\tau}}{\left[\frac{N_R^2}{\tau} + FA_\varepsilon + i_{DC} + F_\beta A_\varepsilon \Omega\right]^{1/2}} = \frac{FA_\varepsilon\sqrt{\tau}}{\left[\frac{N_R^2}{\tau} + N_T\right]^{1/2}} = \frac{FA_\varepsilon\tau}{[N_R^2 + \tau N_T]^{1/2}}.$$

We can obtain the statistical error for the magnitude. While performing photometry in Astroart, SNR (S/N in Figure 7) was calculated and given to us directly. The photometric uncertainties can be calculated using Castro's equation[9]:

$$\sigma_{m_{\text{inst}}} = \frac{2.5}{\ln(10)}\frac{\sigma_I}{I} = \frac{2.5}{\ln(10)}\frac{N}{S} \tag{1}$$

Then we combine the magnitude and its uncertainty into a single table for each filter.

Table 1: AT2023hpb's Magnitude with Uncertainty for filter i

Date (Site)	Magnitude	Uncertainty
May 10 (LSC)	14.257	0.0054
May 11 (LSC)	14.377	0.0058
May 13 (LSC)	14.389	0.0053
May 14 (LSC)	14.380	0.0056
May 15 (LSC)	14.493	0.0059
May 16 (LSC)	14.584	0.0056
May 17 (COJ)	14.901	0.0040
May 18 (LSC)	14.585	0.0055
May 19 (COJ)	14.395	0.0064

Table 2: AT2023hpb's Magnitude with Uncertainty for filter g

Date (Site)	Magnitude	Uncertainty
May 10 (LSC)	14.026	0.0110
May 11 (LSC)	14.190	0.0125
May 13 (LSC)	14.284	0.0095
May 14 (LSC)	14.151	0.0081
May 15 (LSC)	14.238	0.0096
May 16 (LSC)	14.214	0.0077
May 17 (COJ)	14.229	0.0054
May 18 (LSC)	14.238	0.0074
May 19 (COJ)	13.609	0.0078

Table 3: AT2023hpb's Magnitude with Uncertainty for filter r

Date (Site)	Magnitude	Uncertainty
May 10 (LSC)	14.430	0.0045
May 11 (LSC)	14.507	0.0049
May 13 (LSC)	14.549	0.0044
May 14 (LSC)	14.449	0.0044
May 15 (LSC)	14.547	0.0049
May 16 (LSC)	14.666	0.0045
May 17 (LSC)	15.083	0.0031
May 18 (COJ)	14.735	0.0044
May 19 (COJ)	14.267	0.0050

Figure 8-10 are the plots of the magnitude of AT2023hpb with its uncertainties for different filters.

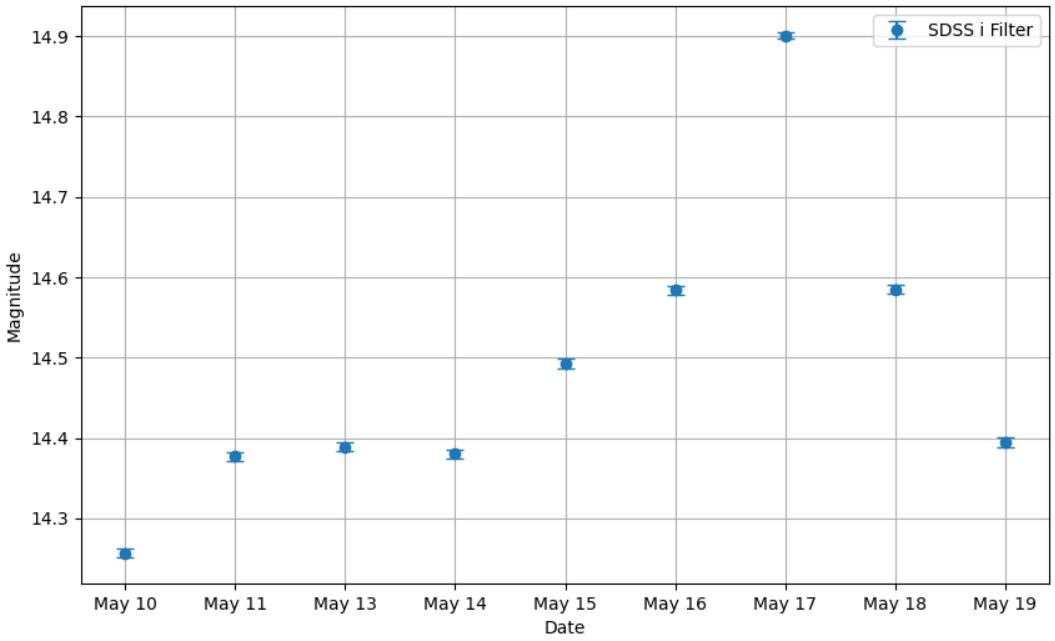

Figure 8: Magnitude of AT2023hpb with Uncertainties for SDSS i Filter

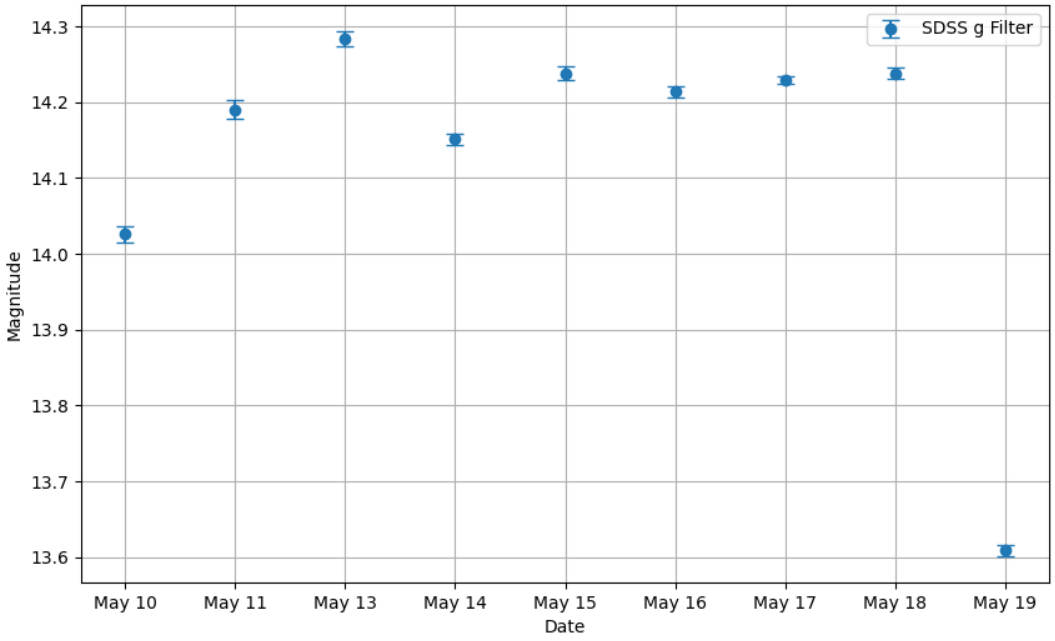

Figure 9: Magnitude of AT2023hpb with Uncertainties for SDSS g Filter

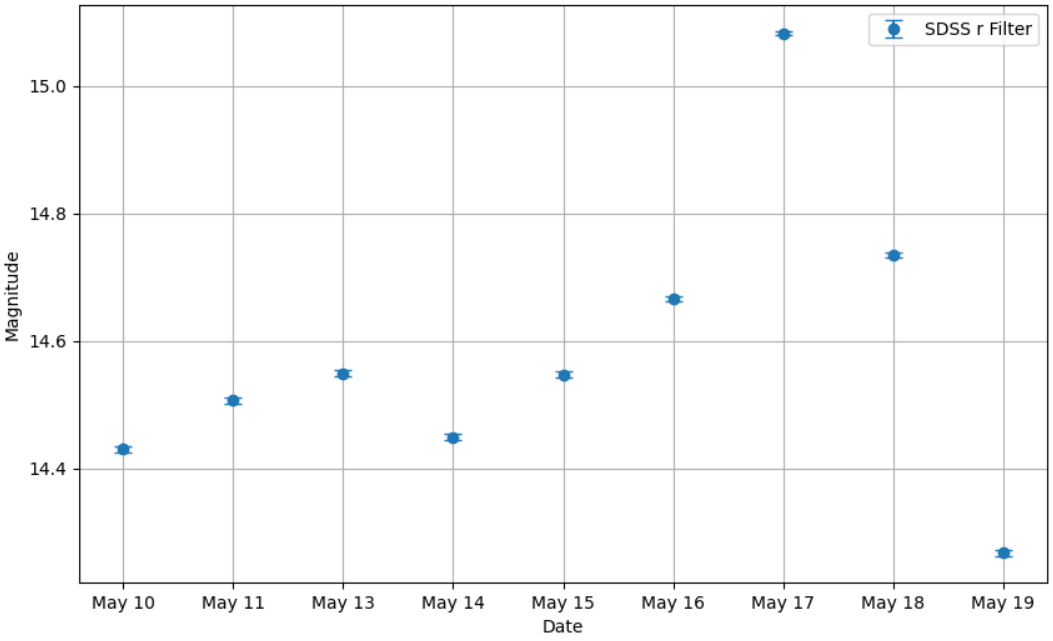

Figure 10: Magnitude of AT2023hpb with Uncertainties for SDSS r Filter

Another plot is created here to combine the magnitude from all 3 filters together and add polynomial fits to each filter. For Figures 8-11, since the lower the magnitude, the brighter the object, the lower the y values, the brighter the object is. Dataset 1 is SDSS i' filter; dataset 2 is SDSS i' filter; dataset 3 is SDSS g' filter.

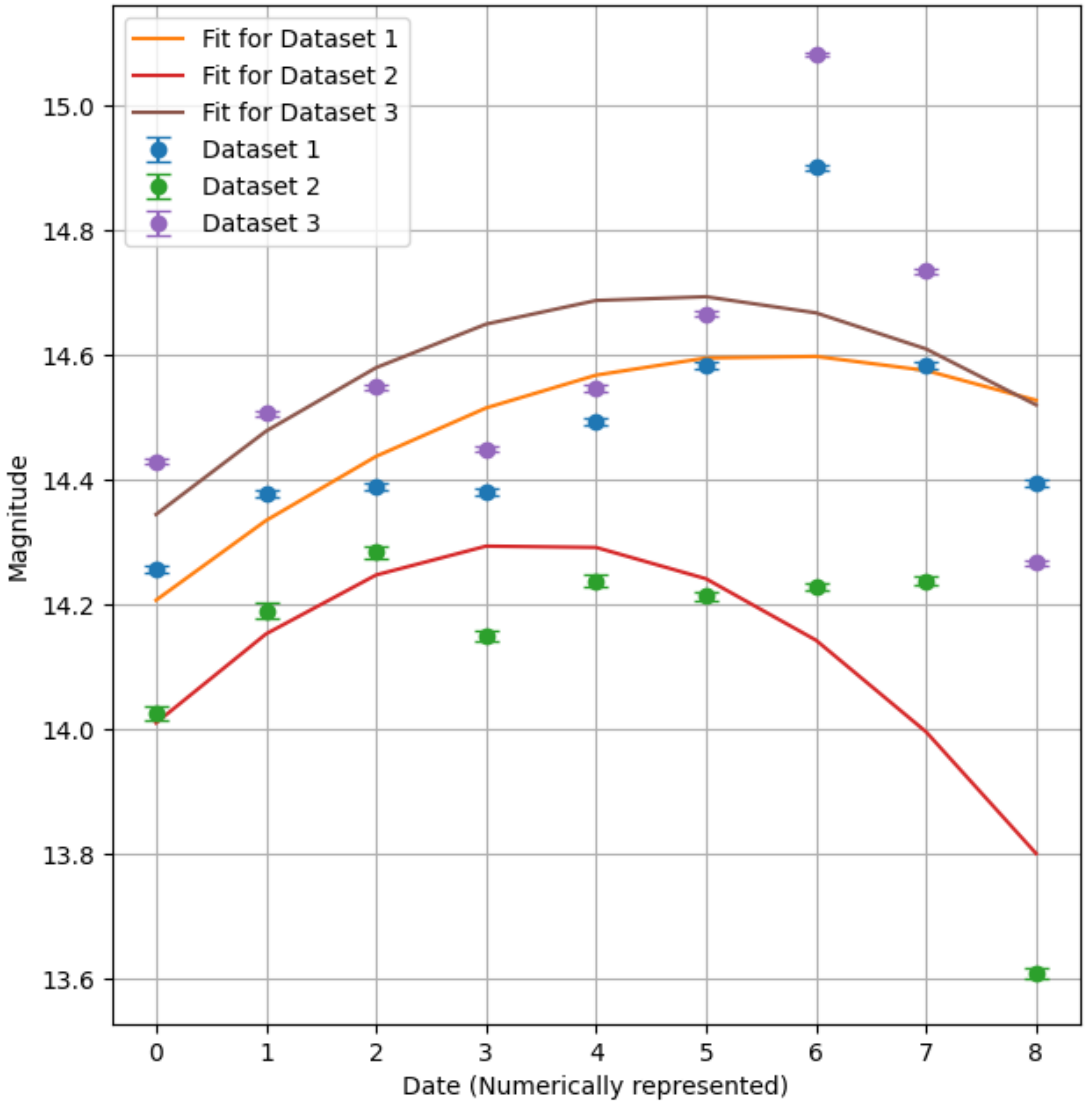

Figure 11: Magnitude of AT2023hpb with Uncertainties for all 3 filters with polyonmial fit lines

Based on Figure 11, we can get some idea about the classification of AT2023hpb. The observed light curves show that it dimed at first, but had a sudden increase in its magnitude. This kind of change is quite unusual, giving the fact that this was a newly discovered supernova. Most supernovae during its early stage would have a constant increase in magnitude, reache its peak, and then gradually dims down. Instead, the data we obtained shows that AT2023hpb has a general pattern of a slow decline for the first eight days, but followed by an increase. In general, it appears brighter on the tenth day than on the first day in the SDSS g' and SDSS r' filters, but the opposite for SDSS i' filter. Moreover, light curves from SDSS i' and SDSS r' filters follow very similar patterns, but the magnitude in SDSS g' filter is noticeably higher in number than that in the other two filters, particularly after the eighth day. This suggests that the supernova emits more light within the SDSS g' frequency range, especially towards the later stage of the observation period. Considering scientists typically track the light curves of a supernova for a period of one to two months to classify its type, it is hard to draw a definite conclusion from our nine-day observational data. However, based on the pattern of the light curver, it is more likely that AT2023hpb is a Type II supernova. Comparing Figure 11 and Figure 1, we can see that the change in magnitude of AT2023hpb is relatively abrupt rather than smooth.

4 Discussion

As discussed in the previoius section, due to the limited length of observation period, we are not certain that AT2023hpb is a Type II supernova. There are several methods we can employ to let us draw a more definite conclusion. Typically, supernovae observations span one to two months; this period extends even further for Type II supernovae due to their slower brightness changes compared to Type I supernovae. Given our short observational window , a clear and regular pattern couldn't be fully established. An intriguing sudden increase in the star's brightness was observed towards the end of our observation period,

where most of our conclusion was drawn from. With more observation time, we could delve deeper into this phenomenon. Another method is to refine our signal-to-noise ratio with extended exposure and image preprocessing, which could bring us a more accurate ligut curve for analysis.

References

[1] Brandi Bernoskie, Heather Deiss, and Denise Miller. What is a supernova?, 2018.

[2] Massimo Turatto. Classification of supernovae. *The Astronomy and Astrophysics Review*, January 2003.

[3] Chapter 21 stellar explosions - university of texas at austin. Online. Accessed on June 5, 2023.

[4] J. B. Doggett and D. Branch. A comparative study of supernova light curves. *Astronomical Journal*, 90:2303–2311, November 1985.

[5] Supernovae - georgia state university. Online, 2003. Accessed on June 5, 2023.

[6] F. Curtis Michel, C. F. Kennel, and William A. Fowler. When will a pulsar in supernova 1987a be seen? *Science*, 238(4829):938–940, 1987.

[7] D. Bodansky, D. D. Clayton, and W. A. Fowler. Nucleosynthesis during silicon burning. *Physical Review Letters*, 20(4):161, 1968.

[8] S. M. Matz, G. H. Share, M. D. Leising, E. L. Chupp, W. T. Vestrand, W. R. Purcell, M. S. Strickman, and C. Reppin. Gamma-ray line emission from sn1987a. *Nature*, 331(6155):416, 1988.

[9] Philip J Castro, Tamara E Payne, Victoria C Frey, Kimberly K Kinateder, and Trenton J Godar. Calculating photometric uncertainty. In *Proceedings of the AMOS Technical Conference*, 2020.